Journal of Ocean Engineering and Marine Energy (2024) 10:85–103
https://doi.org/10.1007/s40722-023-00301-1

RESEARCH

The global techno-economic potential of floating, closed-cycle ocean thermal energy conversion

Jannis Langer[1] · **Kornelis Blok**[1]

Received: 2 May 2023 / Accepted: 25 September 2023 / Published online: 20 October 2023

Abstract

Ocean Thermal Energy Conversion (OTEC) is an emerging renewable energy technology using the ocean's heat to produce electricity. Given its early development stage, OTEC's economics are still uncertain and there is no global assessment of its economic potential, yet. Here, we present the model pyOTEC that designs OTEC plants for best economic performance considering the spatiotemporally specific availability and seasonality of ocean thermal energy resources. We apply pyOTEC to more than 100 regions with technically feasible sites to obtain an order-of-magnitude estimation of OTEC's global technical and economic potential. We find that OTEC's global technical potential of 107 PWh/year could cover 11 PWh of 2019 electricity demand. At $\geq$ 120 MW_{gross}, there are OTEC plants with *Levelised Cost of Electricity (LCOE)* below 15 US¢(2021)/kWh in 15 regions, including China, Brazil, and Indonesia. In the short-to-medium term, however, small island developing states are OTEC's most relevant niche. Systems below 10 MW_{gross} could fully and cost-effectively substitute Diesel generators on islands where that is more challenging with other renewables. With the global analysis, we also corroborate that most OTEC plants return the best economic performance if designed for worst-case surface and deep-sea water temperatures, which we further back up with a sensitivity analysis. We lay out pyOTEC's limitations and fields for development to expand and refine our findings. The model as well as key data per region are publically accessible online.

Keywords Ocean thermal energy conversion · Economic potential · Global analysis · Off-design · Renewable energy

List of symbols

$\dot{Q}$	Heat flow (kW)
$\dot{W}$	Work (kW)
$\dot{m}$	Mass flow (kg/s)
ΔT	Temperature difference (K)
Δp	Pressure drop (Pa)
A	Area (m^2)
a	Availability (%)
b	Scaling coefficient (–)
c	Specific heat capacity (kJ/kgK)
capex	Specific capital expenses (US$(2021)/unit)
CAPEX	Capital expenses (US$(2021)
CRF	Capital recovery factor (–)
d	Inner pipe diameter (m)
f	Friction factor (–)
K	Pressure drop coefficient (–)
l	Pipe length (m)
LCOE	Levelised cost of electricity (US¢(2021)/kWh)
n	Plant lifetime (years)
NTU	Number of transfer unit (-)
OPEX	Operational expenses (US$(2021)/year)
r	Discount rate (%)
T	Temperature (K, °C)
U	Overall heat transfer coefficient (kW/m^2K)
v	Velocity (m/s)
ε	Effectiveness (%)
η	Efficiency (%)
ρ	Density (kg/m^3)
0	Reference
cond	Condensation
CW	Cold deep-sea water
D	Darcy
el	Electric
evap	Evaporation
f	Factor

✉ Jannis Langer
j.k.a.langer@tudelft.nl

[1] Department of Engineering Systems and Services, Faculty of Technology, Policy and Management, Delft University of Technology, Jaffalaan 5, 2628 BX Delft, The Netherlands

gross	Gross
HX	Heat exchanger
hyd	Hydraulic
i	Iteration
in	Inlet
L	Loss
log	Logarithmic
mech	Mechanical
net	Net
out	Outlet
p	Pressure
pipe	Pipe
pump	Pump
t	Technical
trans	Power transmission
turb	Turbine
w	Seawater
WF	Working fluid
WW	Warm surface seawater

1 Introduction

Ocean Thermal Energy Conversion (OTEC) is an emerging renewable energy technology that uses the heat stored in the ocean to produce electricity. Besides OTEC's massive global technical potential of up to 9.3 TW (Jia et al. 2018), benefits over other renewables like solar PV include minimal land use and its baseload character (Vega 2012). Despite this, OTEC still lingers in an early development stage and has not been deployed commercially, yet. One of OTEC's development barriers is its *Capital Expenses (CAPEX)*, which are currently highly uncertain due to lack of data and experience (Langer et al. 2020). This might explain why the existing global OTEC resource potentials reviewed below omit economic aspects and mostly pertain to the theoretical and technical level.

As reviewed by Liu et al. (2020), the most extensive academic work on global OTEC resources has been generated by Nihous et al. Their initial estimation of 3 TW (Nihous 2005) was continuously refined, amongst others with 1° × 1° grid rasterization (Nihous 2007), geographical constraints like distance to coastline (Rajagopalan and Nihous 2013), and an ocean–atmosphere interface (Jia et al. 2018). Using Nihous' (2005) equation for OTEC's power density, Du et al. (2022) found that OTEC's global technical potential might increase by 46% by the end of this century due to the impact of global warming. Other existing resource assessments are limited to regional and national levels, like the Aguni Basin (Liu et al. 2020), Barbados (Hall et al. 2022), and Malaysia (Thirugnana et al. 2021). Besides our earlier work on Indonesia (Langer et al. 2021), we are not aware of any OTEC resource assessments that directly incorporate OTEC's costs into the analysis. Moreover, the studies above only assess OTEC's nominal technical and economic performance, but not the performance under off-design conditions where warm and deep-sea water temperatures deviate from the nominal design values. This aspect has been addressed recently (Giostri et al. 2021; Langer et al. 2022a) showing that seasonal fluctuations in ocean thermal energy resources have a significant impact on the plants' technical and economic performance and thus need to be considered during the design stage. However, both studies used proprietary software and/or data and applied their models on individual plants, but not entire regions. Therefore, it is not clear yet whether their findings apply globally or only locally given the site-specificness of seawater temperature variations.

Against this background, we present a novel Python-based, open-source model, called pyOTEC, which sizes OTEC plants for best economic performance considering spatially and temporally varying ocean thermal energy resources. Using 1 year of daily seawater temperature data in 1/12° × 1/12° (≈ 9 km × 9 km) resolution, we apply pyOTEC to more than 100 countries and territories and calculate more than 150,000 OTEC plants filtered for site selection criteria like water depth, marine protected areas, and exclusive economic zones. Moreover, we check our findings with a sensitivity analysis for key technical and economic inputs. This paper contributes to the academic body of literature in four ways. First, we provide the first estimation of OTEC's global *economic* potential. Second, this paper underlines the significance of spatially and temporally resolved resource data when sizing OTEC plants. Third, we validate the findings of earlier off-design analyses for the entire world and deduce global guidelines for economic OTEC plant sizing. Fourth, pyOTEC delivers spatially explicit time-series data on OTEC's net power production, which can be fed to energy system optimisation models like PyPSA (Brown et al. 2018) and Calliope (Pfenninger and Pickering 2018). With these models, OTEC's role in the global energy transition could be assessed from a system perspective, which is currently unexplored.

The remainder of the paper is structured as follows. Section 2 shows the methods and materials developed and used in this study. Section 3 presents and discusses the findings from our global analysis. The paper ends with conclusions in Sect. 4.

2 Materials and methods

2.1 Theoretical background and overview

Here, we provide the theoretical background for readers unfamiliar with OTEC and a brief overview of the used methods and materials.

OTEC plants are thermal power plants that use warm surface seawater as a heat source and cold deep-sea water as a heat sink. There are many types of OTEC concepts (Vega 2012). Here, however, we only focus on closed-cycle, floating, moored systems. We do not consider onshore OTEC given the differences in plant siting, operations (e.g., water ducting) and cost structure. Nevertheless, we plan to expand pyOTEC for onshore systems in the future.

Following the saturated Rankine cycle, a liquid working fluid (here ammonia) is pumped to the evaporator, where it is fully evaporated using the heat of the surface seawater pumped into the system via seawater pumps. Then, the vapour expands and transfers its energy to the turbine, which drives a generator to produce electricity. The working fluid is fully condensed using cold seawater pumped from the deep sea to the surface. The liquefied fluid flows back to the working fluid pump and the cycle starts anew. All auxiliary equipments, like seawater pumps, are powered by the electricity from the generator. The remaining net power is transmitted from the offshore power plant to the electricity grid onshore via sub-sea cables.

The methods and materials used in this study are visualised in Fig. 1. First, we perform a site selection analysis, during which we remove sites unsuitable for OTEC. Once the user provides the region of interest, pyOTEC downloads the time-series data for surface and deep-sea water temperature [E.U. Copernicus Marine Service Information (CMEMS) 2022]. With these temperature profiles, pyOTEC assesses possible design configurations and for each technically feasible site returns the design with the lowest *Levelised Cost of Electricity (LCOE)* based on a nominal and off-design analysis.

In the following subsections, we describe these steps in more detail.

2.2 Site selection analysis

This subsection is mostly based on our earlier work (Langer et al. 2021). We use the open-source software QGIS 3.18 Zürich (QGIS.org 2023) and datasets listed in Table 1.

First, we span a grid of points across the entire world within a latitude range of 30° N and 30° S (Vega 2012). This range ensures a sufficient temperature difference between surface and deep-sea water of ≥ 20 °C for net positive power production, i.e., power production exceeding seawater pumping power. The points have the same coordinates and spatial resolution ($\approx$ 9 km $\times$ 9 km) as the seawater temperature data to be downloaded later and each point represents one plant. Next, we remove any points that are outside of the regions' exclusive economic zones (Marineregions 2020) considering legal reasons pertaining to the economic use of marine space, but also to ensure a technically and economically feasible distance from plant to shore (Rajagopalan and Nihous 2013). We further remove any points that are inside marine protected areas (UNEP-WCMC 2023a, b, c, d). Moreover, we filter the sites for water depths outside 600–3000 m (GEBCO Bathymetric Compilation Group 2022 2022). The lower end ensures the extraction of sufficiently cold deep-sea water (Vera et al. 2020), while the upper range accounts for the technical limitations of mooring lines. The remaining sites are considered technically feasible for OTEC. Next, we calculate the distance of each site to the closest coastline (QGIS.org 2023) to compute the transmission costs and losses later.

Finally, we calculate the geographic extent of all regions with technically feasible OTEC sites. We store the names of the regions as well as their coordinates in a csv file. This file will be used to download the seawater temperature data as described in the next section. Moreover, we create another csv file that stores all technically feasible OTEC sites (N = 218,481 sites), including their coordinates, region, water depth, and distance to shore. Both csv files are stored in pyOTEC's data inventory and are loaded once the program is initiated.

2.3 The pyOTEC modelling framework

2.3.1 Seawater temperature data

After setting up pyOTEC (see Appendix A), the user is asked for the region and plant size to be analysed. Once these are provided, pyOTEC requests and downloads the time-series data for surface and deep-sea water temperature. In this paper, we use the Global Ocean Physics Reanalysis by Copernicus Marine Service (2022), which offers global ocean data in daily, i.e., 24 h, time steps from 1993 to 2020 in a spatial resolution of 1/12° $\times$ 1/12° ($\approx$ 9 km $\times$ 9 km) across 50 depth layers.

pyOTEC does not download the entire global dataset, but only a part of it, called a subset. The horizontal spatial boundaries of the subset are given by the geographical extent of the analysed region. By default, pyOTEC only requests the seawater potential temperature for the full year 2020 at depths of 21.6 m and 1062 m, which correspond to the length of the warm and cold seawater inlet pipes. The user can change these values in pyOTEC's parameter file. In this paper, we size the plants for four different deep-sea layers (644 m, 763 m, 902 m, and 1062 m) and select for each site the depth with the most economic plant design (i.e., lowest LCOE as described later).

Most likely due to the mismatch of spatial resolution between the seawater temperature and GEBCO bathymetric dataset (500 m $\times$ 500 m versus 9 km $\times$ 9 km), only 162,620 of the 218,481 sites mapped in Sect. 2.2 contain seawater temperature data. These sites are used for the global analysis in this paper.

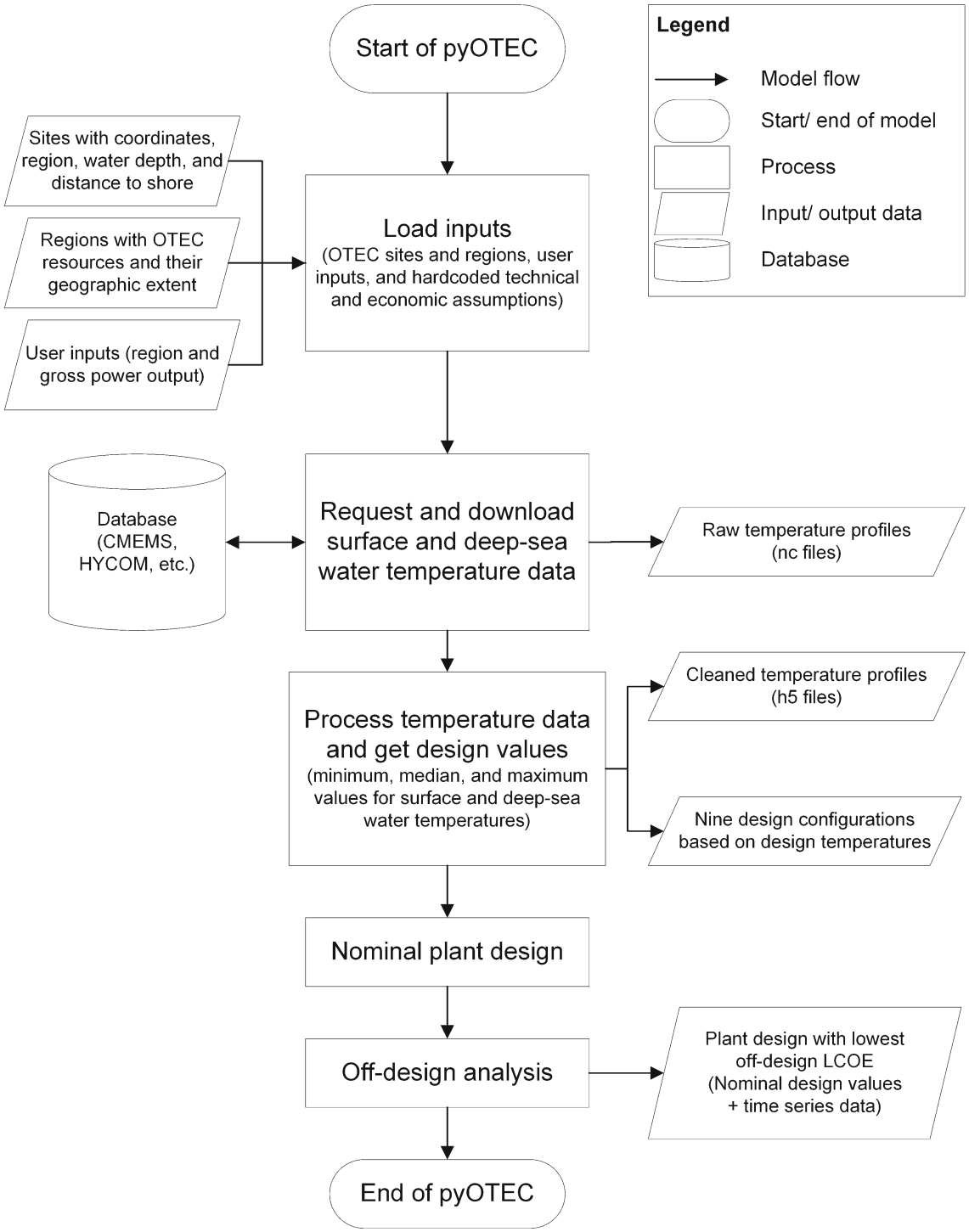

Fig. 1 Flowchart of the pyOTEC model

Before the OTEC plants are sized and analysed, the seawater temperature data are further processed, e.g., cleaned from outliers and NaN. We describe the data processing in more detail in Appendix B.

2.3.2 Nominal and off-design plant sizing

This subsection is based on our earlier off-design OTEC model (Langer et al. 2022a). For this paper, we moved the model from proprietary MATLAB to publicly available Python, fixed bugs, and scaled the model from per-plant

Table 1 Datasets and criteria used for the site selection analysis

Layer	Criterion	Dataset reference	Layer type	Spatial resolution
Climatic zone	30°N–30°S	–	–	–
Exclusive economic zones	Sites must be inside them	(Marineregions 2020)	Vector	–
Marine protected areas	Sites must be outside of them	(UNEP-WCMC 2023a, b, c, d)	Vector	–
Water depth	600–3,000 m	(GEBCO Bathymetric Compilation Group 2022)	Raster	≈ 500 m × 500 m
World map	–	(QGIS.org 2023)	Vector	–

to per-region analysis. Earlier, the model calculated the plant's operation for each time step individually, whereas now pyOTEC performs elementwise arithmetic calculations on the entire time-series data, which is significantly faster. Nonetheless, the underlying equations, assumptions, and system logics from our earlier work (ibid.) remain unchanged, so we summarise the workflow here and refer to the underlying paper for more information.

pyOTEC uses the cleaned seawater temperature data to calculate the site-specific minimum, median, and maximum surface and deep-sea water temperatures. These temperatures are used to perform a two-stage design process consisting of a nominal and off-design analysis using the technical assumptions listed in Table 2. All inputs are stored in one separate parameter file and can be changed by the user.

First, the OTEC plants are sized under nominal conditions, meaning that the plants are assumed to operate solely under design conditions without seasonal seawater temperature variations. The plants are designed using combinations of minimum, median, and maximum warm and cold seawater temperatures as inlet temperatures for the evaporator and condenser. In this paper, we call these nine combinations of warm and cold inlet temperatures *configurations* as visualised in Fig. 2. To determine the economically best nominal outlet temperatures, pyOTEC loops through 49 combinations of warm and cold seawater temperatures differences between inlet and outlet (from 2 °C to 5 °C in steps of 0.5 °C). For example, if the nominal warm and cold inlet temperatures are 28 °C and 4 °C, then the assessed nominal warm and cold outlet temperatures range between 23 and 26 °C (28 °C minus 5 °C and 28 °C minus 2 °C) and 6 and 9 °C (4 °C plus 2 °C and 4 °C plus 5 °C) in intervals of 0.5 °C.

For all inlet and outlet temperature combinations, pyOTEC deploys the following workflow. Using the outlet temperatures and pinch-point temperatures, pyOTEC calculates the nominal saturation pressures and temperatures of the working fluid in the evaporator and condenser. With these and the gross turbine work $\dot{W}_{t,\,gross}$ provided by the user (entered as a negative number according to IUPAC sign convention), the enthalpies, working fluid and seawater mass flows, as well as heat flows and working fluid pump work are calculated. Next, the evaporator and condenser are sized using Eq. (1), where $\dot{Q}_{HX}$ is the heat flow, U_{HX} is the overall heat transfer coefficient, and $\Delta T_{log,\,HX}$ is the logarithmic mean temperature difference of the heat exchanger HX

$$A_{HX} = \frac{|\dot{Q}_{HX}|}{U_{HX} * \Delta T_{log,\,HX}}. \tag{1}$$

Next, the seawater pipes and pumps are sized. The number and inner diameter of the pipes of the warm and cold system side are calculated, such that the maximum allowed inner diameter (default: 8 m) and pressure drop (default: 100 kPa) are not exceeded, mainly by tuning the nominal seawater velocity. We assume that the warm and cold seawater mass flows are distributed evenly across their respective warm and cold seawater pipes. The total pressure drop in the warm and cold system side is calculated using Eq. (2), where Δp_w is the total pressure drop, $f_{D,w}$ is the Darcy friction factor, ρ_w is the seawater density, $l_{pipe,\,w}$ and $d_{pipe,\,w}$ are the total length and inner diameter of the pipes, $v_{pipe,w}$ and $v_{HX,w}$ are the velocities in the pipes and heat exchanger, respectively, and $K_{L,w}$ is the pressure drop coefficient for the heat exchanger HX. Index w distinguishes the warm and cold system side

$$\Delta p_w = \rho_w * \left(f_{D,\,w} * \frac{l_{pipe,\,w}}{d_{pipe,\,w}} * \frac{v_{pipe,\,w}^2}{2} + K_{L,\,w} * \frac{v_{HX,\,w}^2}{2} \right). \tag{2}$$

The required seawater pump work $\dot{W}_{t,\,pump,\,w}$ per system side w is calculated with Eq. (3), using the seawater mass flow $\dot{m}_w$ and the hydraulic and electric seawater pump efficiencies $\eta_{pump,\,hyd}$ and $\eta_{pump,\,el}$

$$\dot{W}_{t,\,pump,\,w} = \frac{\dot{m}_w * \Delta p_w}{\rho_w * \eta_{pump,\,hyd} * \eta_{pump,\,el}}. \tag{3}$$

The net power at shore $\dot{W}_{t,\,net}$ is computed with Eq. (4), where $\eta_{turb,\,mech}$ and $\eta_{turb,\,el}$ are the mechanical and electric turbine efficiency, $\dot{W}_{t,\,pump}$ is the pumping power of the cold and warm system side CW and WW as well as the working fluid WF, and the power transmission efficiency from floating OTEC plant to shore η_{trans}. Note that the work

Table 2 Technical assumptions for the nominal and off-design analysis

Parameter	Assumption	Reference(s)
Density liquid ammonia [kg/m^3]	625	
Spec heat capacity seawater [kJ/kgK]	4.0	(Sharqawy et al. 2011)
Density surface seawater [kg/m^3]	1024	(Upshaw 2012)
Density deep seawater [kg/m^3]	1027	(Upshaw 2012)
Pinch-point temperature difference evaporator and condenser [K]	1.0	(Bharathan 2011; Sinnott and Towler 2022)
Nom overall heat transfer coefficient evaporator [kW/m^{2}K]	4.5	(Bernardoni et al. 2019; Giostri et al. 2021)
Nom overall heat transfer coefficient condenser [kW/m^{2}K]	3.5	(Martel et al. 2012; Giostri et al. 2021)
Isentropic efficiency turbine [%]	82	(Vera et al. 2020)
Mech efficiency turbine [%]	95	(Soto and Vergara 2014; Vera et al. 2020)
Electrical efficiency generator [%]	95	(Soto and Vergara 2014; Vera et al. 2020)
Hydraulic efficiency seawater pump [%]	80	(Vera et al. 2020; Giostri et al. 2021)
Electric efficiency seawater pump [%]	95	(Giostri et al. 2021)
Mech efficiency ammonia pump [%]	95	(Giostri et al. 2021)
Isentropic efficiency ammonia pump [%]	80	(Vera et al. 2020)
Default length inlet WW pipe [m]	21.6	
Default length inlet CW pipe [m]	1,062	
Length outlet WW and CW pipe [m]	60	
Pipe thickness [m]	0.09	(Cable 2010; Vega and Michaelis 2010)
Density HDPE [kg/m^3]	995	(Cable 2010)
Roughness factor z [mm]	0.0053	(Vera et al. 2020)
Pressure drop coefficient evaporator and condenser [–]	100	
Nominal flow velocity in the pipes [m/s]	2.0	(Vega 2012; Bernardoni et al. 2019)
Nominal flow velocity in the heat exchangers [m/s]	1.0	(Bernardoni et al. 2019)
Maximum inner pipe diameter [m]	8	

Except for the seawater inlet pipe lengths, all assumptions are directly taken from (Langer et al. 2022a). Note that the pressure drop coefficient for evaporator and condenser was accidentally given as 120 in the earlier study (ibid.), although it should be 100. [–] refers to unitless parameters

flows are aggregated, because the turbine work has a negative sign, while the pump works have positive signs following the IUPAC sign convention:

$$\dot{W}_{t,net} = \frac{\dot{W}_{t,gross} * \eta_{turb,mech} * \eta_{turb,el} + \dot{W}_{t,pump,CW} + \dot{W}_{t,pump,WW} + \dot{W}_{t,pump,WF}}{\eta_{trans}}. \tag{4}$$

With the plants being sized, pyOTEC calculates the component *Capital Expenses (CAPEX)* using the economic assumptions in Table 3. OTEC's strong economies of scale are accounted for with Eq. (5). Where applicable, the specific component cost *capex* of a plant with the user-defined size $\dot{W}_{t,gross}$ are scaled against a reference plant of size $\dot{W}_{t,gross,0}$, component cost $capex_0$ and scaling exponent b. The user can select between *low-cost* and *high-cost* assumptions reflecting the high uncertainty of OTEC's cost (Langer et al. 2020). By default, pyOTEC uses the low-cost assumptions and the results presented here pertain to them

$$capex = capex_0 * \left(\frac{\dot{W}_{t,gross,0}}{\dot{W}_{t,gross}}\right)^b. \tag{5}$$

After summing up all component CAPEX to form the total system CAPEX, we move to the *Levelised Cost of Electricity (LCOE)*, which reflects the costs of electricity generation considering all costs in their present value accruing over the

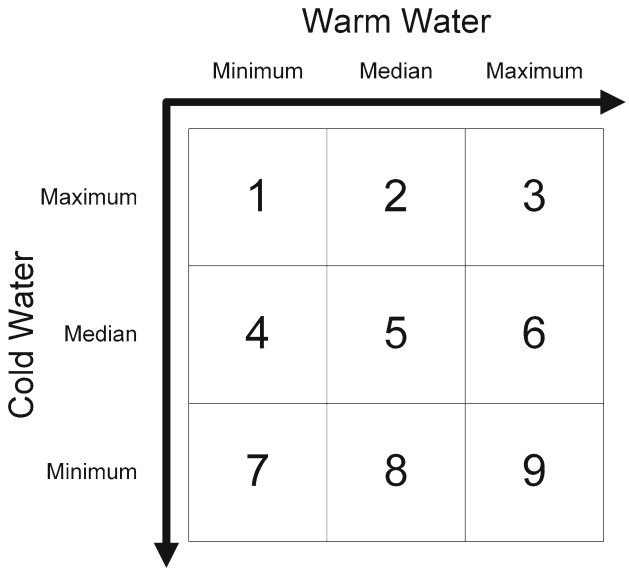

Fig. 2 The nine configurations analysed by pyOTEC (modified illustration from Langer et al. (2022a)). Configuration 1 is the most conservative design based on worst-case temperature values, whereas configuration 9 is the most optimistic design using best-case temperature values

plant's lifetime. First, we calculate the *Capital Recovery Factor (CRF)* with Eq. (6) to annualise the total system CAPEX, using the discount rate r and useful lifetime n. The LCOE is computed with Eq. (7), using CRF, total system CAPEX, *Operational Expenses (OPEX)*, net power $\dot{W}_{t,net}$, and the availability factor a_f reflecting how long the plant operates per year after planned and unplanned downtime

$$CRF = \frac{r*(1+r)^n}{(1+r)^n-1} \tag{6}$$

$$LCOE = \frac{CAPEX*CRF+OPEX}{\dot{W}_{t,net}*a_f*8,760\frac{hours}{year}}. \tag{7}$$

The output of Eq. (7) is the nominal LCOE, which assumes that the nominal design conditions, including seawater temperatures, apply continuously throughout the plants' lifetime. The nominal LCOE is calculated for each of the possible 49 outlet temperature combinations to find the plant design with the lowest nominal LCOE. That design, together with its properties, e.g., heat exchanger areas, are passed to the off-design analysis module.

The goal of the off-design analysis is to find the configuration from Fig. 2 with the lowest LCOE considering the seasonal variations of warm and cold ocean thermal energy

Table 3 Low-cost economic assumptions taken from Langer et al. (2022a) used in this study

Cost component	Specific reference cost $capex_0$ [Ref]	Scaling exponent b [-]	Reference gross power $P_{gross,0}$ [MW]	References
Turbine [US$/kW$_{gross}$]	328	0.16	136	(Cable 2010; Martel et al. 2012)
Heat exchangers [US$/m^2]	226	0.16	80	(Cable 2010; Vega 2010; Upshaw 2012)
Pumps [US$/kW$_{pump}$]	1674	0.38	5.6	(Vega 2010; Upshaw 2012)
Seawater pipes [US$/kg$_{pipe}$]	9	–	–	(Cable 2010; Bernardoni et al. 2019)
Power transmission [US$/kW$_{gross}$]	$10.3 * D + 68.7$	–	–	(Bosch et al. 2019)
Design & management [US$/kW$_{gross}$]	3,113	0.70	4.0	(Martel et al. 2012; Bernardoni et al. 2019)
Structure & mooring [US$/kW$_{gross}$]	4,465	0.35	28.1	(Martel et al. 2012; Upshaw 2012)
Deployment [US$/kW$_{gross}$]	650	–	–	(Martel et al. 2012)
Extra costs [% of CAPEX]	5	–	–	(Cable 2010)
OPEX [% of CAPEX/year]	3	–	–	(Vega 2010)
Project lifetime n [years]	30			(Langer et al. 2020)
Discount rate r [%]	10			(Langer et al. 2021)
Availability factor a_f [%]	91.3			(Jung et al. 2016; Bernardoni et al. 2019)

The variable D for power transmission costs refers to the distance from the OTEC plant to the closest coastline. All costs are displayed in US$(2021) values

resources. The major difference between the nominal and off-design analysis is that the latter does not use nominal temperatures, but time-series data, which is not equal to the nominal temperatures most of the times. Hence, there can be a lack and/or excess of warm and/or cold ocean thermal energy resources.

To account for these situations, we use the sliding pressure control logic from our earlier model (Langer et al. 2022a). With this logic, the evaporation pressure is decreased if the warm seawater temperature is below the nominal temperature; and the condensation pressure is increased if the cold seawater temperature is above the nominal temperature. If there is an excess of warm and/or cold ocean thermal energy resources, the evaporation and/or condensation pressures are kept at nominal values, and instead, the seawater mass flows are decreased, as less seawater is required to evaporate/condense the same amount of working fluid. The (adjusted) saturation pressures and temperatures as well as enthalpies at each process stage are calculated with the same equations as for the nominal analysis.

In case of excess, pyOTEC accounts for the off-design behaviour of the heat exchangers using Eqs. (8–12). There, the Number of Transfer Unit NTU, effectiveness ε_{HX} (assuming single-flow heat exchange), outlet temperature $T_{w,out}$, seawater mass flow $\dot{m}_w$, and overall heat transfer coefficient U_{HX} are solved iteratively over i iterations for heat exchanger HX and system side w. Assuming plate heat exchangers, the scaling exponent for U_{HX} against the nominal values nom is 0.65 (Sinnott and Towler 2022)

$$NTU_{HX,i} = \frac{U_{HX,i} * A_{HX}}{\dot{m}_{w,i} * c_p} \tag{8}$$

$$\varepsilon_{HX,i} = 1 - e^{-NTU_{HX,i}} \tag{9}$$

$$T_{w,out,i} = \begin{cases} T_{w,in} - \varepsilon_{HX,i} * \left(T_{w,in} - T_{evap}\right) if\ evaporator \\ T_{w,in} + \varepsilon_{HX,i} * \left(T_{cond} - T_{w,in}\right) if\ condenser \end{cases} \tag{10}$$

$$\dot{m}_{w,i+1} = \frac{-\dot{Q}_{HX}}{c_p * (T_{w,out} - T_{w,in})} \tag{11}$$

$$U_{HX,i+1} = U_{HX,nom} * \left(\frac{\dot{m}_{w,i+1}}{\dot{m}_{w,nom}}\right)^{0.65} \tag{12}$$

$$repeat\ until \left|(T_{w,i+1} - T_{w,i})\right| < 1E^{-7}$$

$$for\ i = 0 \rightarrow U_{HX,i} = U_{HX,nom}\ and\ \dot{m}_{w,i} = \dot{m}_{w,nom}.$$

For the system pressure drop Δp_w, seawater pumping power $\dot{W}_{t,\,pump,\,w}$, and net power $\dot{W}_{t,net}$, we again use Eqs.(2–4), but this time with the time-series data as inputs.

The off-design LCOEs per configuration are calculated using Eq. (7), this time using the average net power output throughout the modelled time span. After the nominal and off-design analyses are conducted for all nine configurations, pyOTEC returns the configuration with the lowest off-design LCOE.

2.4 Global analysis and sensitivity analysis

To test the model and showcase its usefulness, we apply pyOTEC to all countries and territories with technically feasible OTEC sites and available electricity demand data. To assure an adequate size of the plants in relation to electricity demand, we calculate the plant size by dividing the regions' 2019 net electricity consumption (EIA n.d.) by 8760 h per year. The maximum plant size is capped at 136 MW_{gross}, which represents OTEC at full commercial size with limited further economies of scales (Vega 2012). The index 'gross' refers to the power output of the turbine excluding losses and the power consumption of auxiliary equipment. If the electricity demand of a region is not listed, the region is omitted from the analysis.

The approach above is strongly simplified and merely yields an order-of-magnitude estimation of OTEC's global economic potential. With this approach, we disregard demand covered by existing and future competing power generation technologies. Therefore, regions highlighted as relevant in this study should be further investigated with more localised and refined data.

Furthermore, we perform a sensitivity analysis to consolidate the key findings of this paper. We change each key technical and economic parameter by ± 30% (where possible) and record the changes in LCOE and configuration. Since this analysis comprises dozens of re-runs, we perform the analysis only for Indonesia, which we deem as representative given the country's diversity of ocean thermal energy resources.

2.5 Methodological limitations

This section discusses the four main limitations of pyOTEC. First, the model's scope is currently limited to floating, closed-cycle OTEC using plate heat exchangers and ammonia as working fluid. Alternative concepts (e.g., open-cycle OTEC as well as Kalina and Uehara cycle), technologies, and working fluids are consequently omitted. Second, the plants' operation is simplified as we neglect aspects like heat transfer in the seawater pipes and pumps as well as deteriorating system performance due to biofouling. Regarding plant spacing, we do not consider location-specific limitations like the availability of cold deep-sea water from global ocean currents (Ascari et al. 2012) and other uses of marine space, like shipping. Third, although economically feasible systems can be designed with pyOTEC, the results are not optimised as optimal configurations do not necessarily pertain to minimum, median, or maximum values. This limitation could

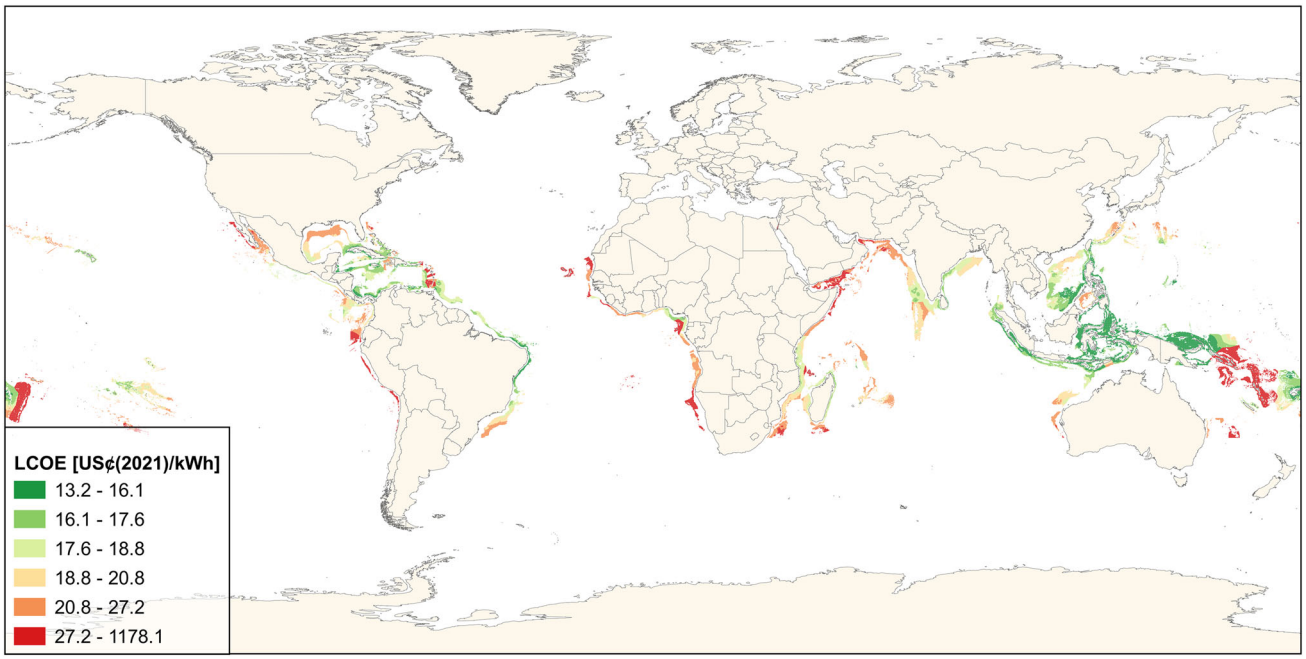

Fig. 3 OTEC sites ($N = 162{,}620$ sites) across the world and their LCOEs

be addressed with an interpolation map, which we did not do here to limit computational costs of the global analysis. Fourth, pyOTEC's economic model is based on current knowledge of OTEC economics, which is limited due to the technology's early development stage.

All these limitations considered, there are ample fields of development for pyOTEC, and we hope that this paper motivates other OTEC researchers to participate in the model's improvement. Regardless, the above-mentioned limitations do not diminish the model's usefulness as a pre-feasibility study tool.

3 Results and discussion

3.1 Global OTEC resources and their LCOEs

Figure 3 shows all technically feasible OTEC sites and their LCOEs. Economically interesting sites with LCOEs below 17.6 US¢(2021)/kWh are mostly situated along the equator in South-East Asia and South America. At higher latitudes, LCOEs increase due to fewer ocean thermal energy resources and higher seasonal variability. Some sub-tropical regions in the Caribbean Sea and Asia are exceptions with LCOE below 17.6 US¢(2021)/kWh, as well. In Africa, East Asia, and Australia, LCOEs tend to be higher, either due to small plant sizes with lower economies of scale (e.g., Liberia), comparatively low surface seawater temperatures (e.g., in Australia), or high deep-sea water temperatures (e.g., in India). Nonetheless, interesting cases for large-scale OTEC with LCOE below 20 US¢(2021)/kWh can still be found in India and Africa (e.g., in Nigeria).

Out of the 162,620 analysed sites, 81% yielded the lowest LCOE at a deep-sea water intake of 1,062 m. A longer cold water pipe increases pipe costs and pumping power. However, the lower deep-seawater temperatures allow for fewer cold water pipes with smaller diameters as less water is required to condense the same amount of working fluid. Together with the downsizing of other cold-side components, like condenser, the benefits of deeper cold water intake outweigh the drawbacks in our model.

Table 4 shows the 20 regions with largest technical potential for OTEC and their 2019 electricity demand coverage. The technical potential depends on the system size, available marine area suitable for OTEC, plant spacing, and warm and cold ocean thermal energy resources. For most regions, there is a mismatch between OTEC supply and electricity demand, with regions where supply exceeds demand by a manifold, like Fiji, and regions where OTEC could only meet parts of demand, e.g., in China and the United States. If OTEC's economic potential is limited by 2019 demand, only 11 PWh/year of the global technical potential of 107 PWh/year would be tapped economically unless future grid expansions allow for the long-distance transport of OTEC power across land and sea.

Note though that the technical potential of 107 PWh/year does not reflect how much OTEC could and should be implemented in practice. First, such a level of deployment might entail significant environmental impacts on local ecosystems, e.g., via ocean thermal degradation. With a simplified

Table 4 The 20 regions with the largest OTEC resources and their potential to cover 2019 net electricity consumption

Region	Total technical OTEC potential [TWh/year]	System size per plant [MW_{gross}]	Net electricity consumption in 2019 [TWh]	Economic potential [TWh/year] if capped by		Total marine area [10^3 km^2]	Marine area occupied by OTEC [10^3 km^2] and [%]	Electricity generation density [GWh/km^2]	Warm seawater temperatures [°C]			Cold seawater temperatures [°C]		
				2019 demand	Two times 2019 demand				Min	Med	Max	Min	Med	Max
Indonesia	14,119	136	255	255	509	6,029	1,357 (22%)	10.41	21.1	29.3	31.7	2.3	4.6	13.4
Papua New Guinea	8,980	136	4.1	4.1	8.3	2,403	860 (36%)	10.44	24.8	30.1	31.6	3.1	4.2	7.7
India	7,437	136	1,342	1,342	2,684	1,660	753 (45%)	9.88	23.8	29.2	31.6	4.6	7.2	11.7
Fiji	6,382	120	1.1	1.1	2.1	1,284	714 (56%)	8.94	21	27.5	30.8	2.8	3.8	7.8
Brazil	5,142	136	538	538	1,076	3,208	521 (16%)	9.87	18.5	26	30.1	2.9	3.9	8.1
Philippines	4,208	136	96	96	192	1,974	412 (21%)	10.21	22.8	29.3	31.9	2.1	4.2	10.9
Mexico	3,853	136	279	279	558	3,181	444 (14%)	8.69	12.5	26.5	32.2	3.6	4.7	8.6
Japan	3,396	136	945	945	1,890	4,065	368 (9%)	9.22	18.8	25.6	31.5	2.5	3.7	8.7
United States	3,286	136	3,989	3,286	3,286	2,450	372 (15%)	8.84	18.2	26	31	3.1	4.8	14.6
Mozambique	3,158	136	13.5	13.5	26.9	567	318 (56%)	9.94	19.7	26.9	30.7	2.9	5.9	12.1
Australia	3,116	136	239	239	477	6,866	343 (5%)	9.09	17.1	26.6	31.8	3.4	4.9	8.6
Madagascar	2,854	136	1.9	1.9	3.8	1,194	295 (25%)	9.67	19.4	26.9	31.6	2.4	5.5	12.5
French Polynesia	2,656	73	0.64	0.64	1.3	4,772	498 (10%)	5.33	18.5	27.7	30	3.2	4	6.7
Vietnam	2,289	136	213	213	426	751	227 (30%)	10.09	22.9	28.7	31.5	3.6	4.1	7.4
Republic of Mauritius	2,077	136	2.9	2.9	5.8	1,279	215 (17%)	9.65	21.7	26.2	30.5	4.1	5	9.7
China	1,959	136	6,803	1,959	1,959	1,307	196 (15%)	9.99	22.9	27.8	31.4	3.5	4.1	6.8
Costa Rica	1,792	136	10	10	20	590	187 (32%)	9.60	15.3	26.8	30.7	3.4	4.5	7.4
Jamaica	1,603	136	3.1	3.1	6.2	272	159 (59%)	10.06	26.5	28.4	30.6	4.4	5	10
Colombia	1,532	136	74	74	148	718	167 (23%)	9.15	14.2	27.3	30.5	3.9	4.9	8.8
Maldives	1,511	70	0.62	0.62	1.2	921	289 (31%)	5.24	27	29.3	31.4	5	6.6	10.8
World	107,012	–	23,921	10,974	16,222	105,702	13,172 (11.9%)	8.1	–	–	–	–	–	–

The countries and regions are ordered by descending total OTEC electricity generation. "Total marine area" for the world refers to the marine areas (i.e., exclusive economic zones) of countries and territories with OTEC resources. "Marine area occupied by OTEC" does not refer to the area of the floating OTEC platform, but the assumed spacing of 9 km × 9 km between plants

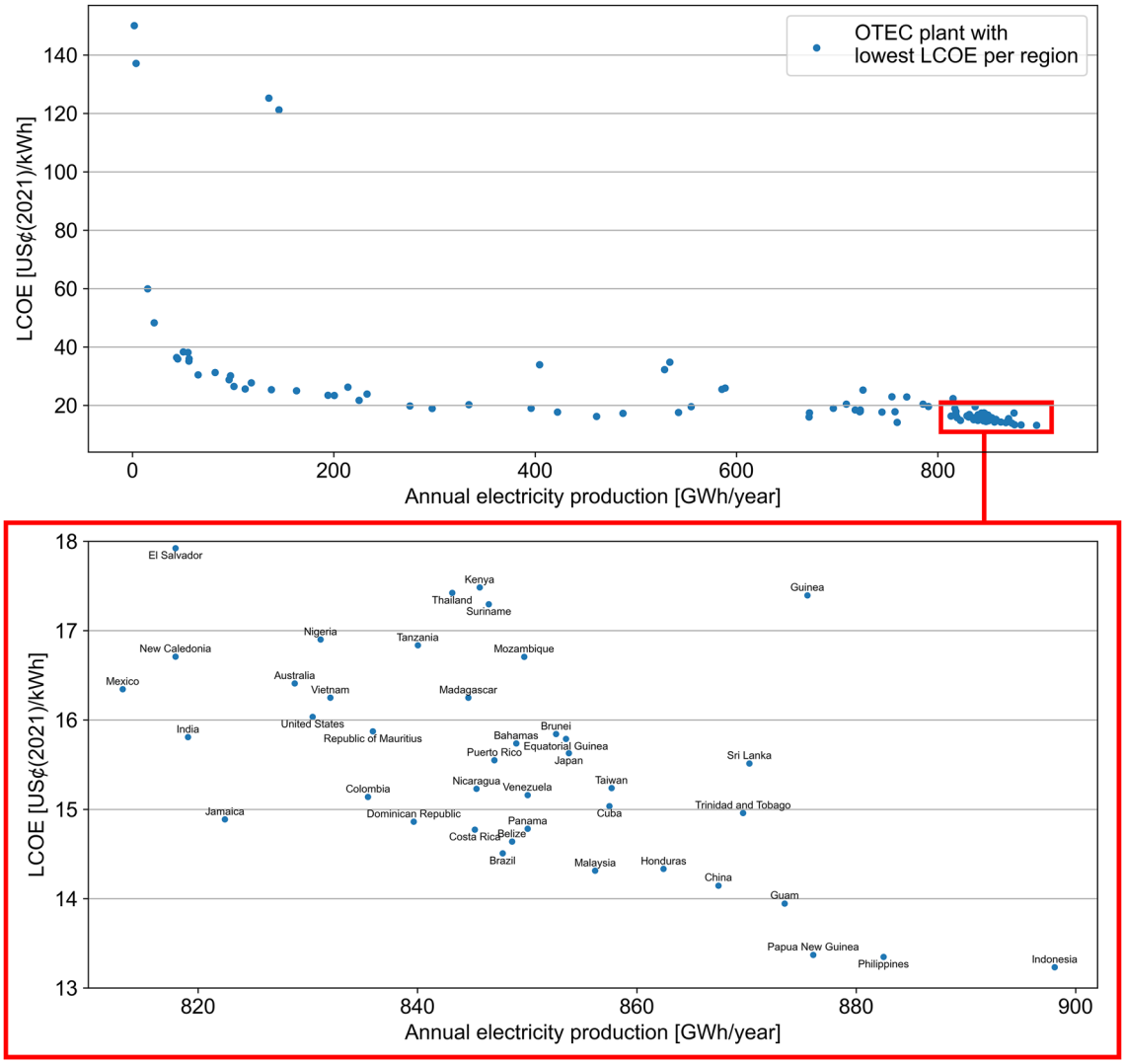

Fig. 4 The OTEC plants with the lowest off-design LCOE per region and their respective annual electricity production. The bottom portion of the figure (red frame) zooms onto a set of interesting countries and territories with LCOE < 18 US¢(2021)/kWh and annual electricity production > 800 GWh/year

uniform plant spacing of 9 km × 9 km, we disregard the location-specific availability of cold deep-sea water from global ocean currents, which might necessitate a further spacing of plants (Ascari et al. 2012). Other environmental pressures by OTEC include the relocation of toxic materials as well as entrainment (i.e., organisms entering the water intake) and impingement (i.e., organisms being caught at screening structures at the water intake) (Hammar et al. 2017). Second, there might also be negative economic implications, e.g., from the adjustment of shipping routes to avoid collisions between ships and OTEC plants. Then again, such widespread implementation would not be necessary in most regions. Countries like Fiji could meet their electricity demand with a single OTEC plant, which would only require 0.006% of available marine area. Even large countries like Indonesia would only need 0.4% of available marine area to fully meet their 2019 electricity demand. Hence, we would expect OTEC's environmental impact to be moderate in such regions. In countries like China and the United States, where the technical OTEC potential is less than demand, we would see OTEC more as a complimentary technology to other renewables (see Sect. 3.2).

Figure 4 shows the lowest LCOE per region and the electricity production of the corresponding plants. The LCOE is not only tied to resource availability, but also plant size given OTEC's economies of scale. Our results show that LCOEs below 20 US¢(2021)/kWh are possible at plant sizes as small as 44 MW_{gross} (Haiti). As shown in the bottom part of Fig. 4, LCOEs below 15 US¢(2021)/kWh are achieved in 15 regions

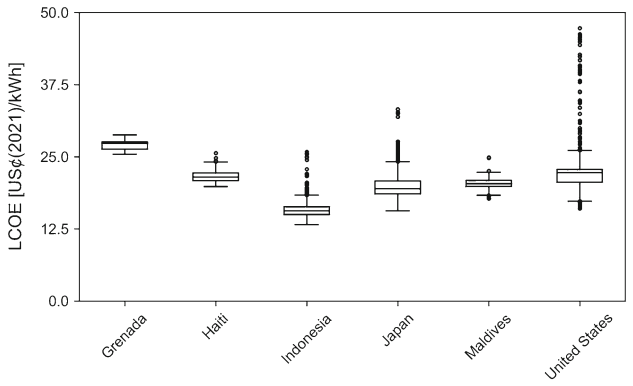

Fig. 5 Box and whisker plots showing ranges of LCOE across selected countries and system sizes (Grenada: 22 MW_{gross}, Haiti: 44 MW_{gross}, Maldives: 70 MW_{gross}, rest 136 MW_{gross}). Outliers are points outside 1.5 times the interquartile range

at system sizes $\geq$ 120 MW_{gross}. Therefore, OTEC at full scale could be an economically attractive alternative to other renewables in high-demand countries, especially considering further cost reductions via global technological learning (Langer et al. 2022b).

Then again, there are many cases where large-scale OTEC is neither economically sensible nor necessary. Upscaling only marginally improves OTEC's economic feasibility if local ocean thermal energy resources are generally low. Good examples are Egypt and Saudi Arabia, where the minimum LCOEs of 136 MW_{gross} systems are 125 and 121 US¢(2021)/kWh, respectively. Moreover, full-scale OTEC might not be necessary for small island developing states. There, electricity demand is too low for such systems; high electricity generation costs might allow smaller systems to be economic. For example, the 7.1 MW_{gross} systems in Tonga can have LCOEs as low as 36.4 US¢(2021)/kWh, which is significantly lower than the estimated total generation cost of more than 100 US¢(2016)/kWh in the off-grid parts of the island (Asian Development Bank 2016). Hence, OTEC's path towards commercialisation and full scale could begin at such island states, which would benefit from a stable, clean, and cheaper electricity supply.

Figure 5 shows how the LCOE can vary within the analysed regions. While the variations are rather small in Grenada, Haiti, and the Maldives, they are considerable in Indonesia, Japan, and the United States. This can mainly be explained by the extent of the regions. The marine area of Grenada, for example, is comparatively small, so ocean thermal energy resources and the distance from OTEC plant to shore are relatively uniform. In contrast, countries like Indonesia and United States stretch over thousands of kilometres, so ocean thermal energy resources can be quite diverse. These things considered, one must be aware of the potentially significant fluctuations of LCOE.

3.2 OTEC's potential role against other renewables

In practice, OTEC's economic potential also depends on its competitiveness against other renewables. According to IRENA (2022), all major renewable energy technologies except concentrated solar power reached global weighted LCOE $\leq$ 7.5 US¢(2021)/kWh in 2021 (i.e., bioenergy, geothermal, hydropower, solar PV, and onshore and offshore wind). Regarding other ocean energies, IRENA (2020) reports current LCOEs of 20–45 US¢/kWh for tidal energy and 30–55 US¢/kWh for wave energy, which are expected to decline to 11 US¢/kWh and 16.5 US¢/kWh, respectively, until 2030.

Unless costs decline substantially, OTEC would not be able to undercut its (more mature) competitors' costs. Therefore, why should OTEC be considered if there are significantly cheaper and commercially available alternatives?

We believe that small island developing states and archipelagic states are the most interesting niches for OTEC. Especially, the former are currently strongly dependent on expensive imported Diesel from volatile global markets (Michalena and Hills 2018). Unless these islands have geothermal resources (International Renewable Energy Agency and International Geothermal Association 2023), their options for Diesel generator substitution with renewables are limited. Regarding bioenergy, fuel dependency would shift from Diesel to biofuels if imported, and domestically cultivated power crops would compete against food crops and other land uses (Michalena and Hills 2018). The latter issue might also be relevant for hydropower, solar PV, and onshore wind. Regarding offshore wind, there are islands, like Sao Tome and Principe, where mean wind speeds are too low for an economic operation of currently available offshore wind turbines (DTU Wind Energy et al.). On islands with economic offshore wind and/or geothermal potentials, we see OTEC as a complimentary technology that diversifies the islands' electricity generation mix. Once developed towards maturity within these niches, OTEC might become an interesting technology for continental coastal states, as well. There, OTEC could substitute the final bits of fossil-fuel-based power generation that would otherwise require large capacities of solar PV, wind power, and/or energy storage. Moreover, OTEC could also be considered for its dispatchability, especially once the penetration of non-dispatchable renewables, like solar PV, increases.

Note that this discussion solely pertains to floating, closed-cycle OTEC. Further economic potentials could arise from onshore OTEC if there is trade-off between avoiding mooring and platform costs on the one side and increased pipe costs and pumping power on the other. Furthermore, there are plenty of other concepts and use cases discussed in the literature, e.g., freshwater and power production via open-cycle OTEC (Vega 2012), the production of e-fuels like hydrogen

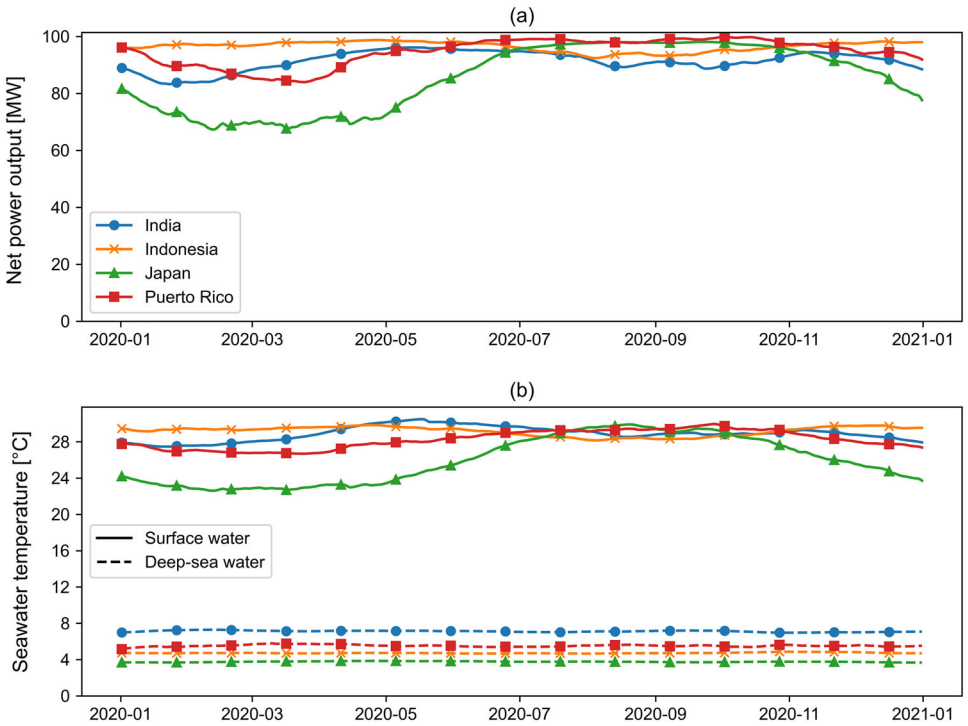

Fig. 6 Time-series data for four example countries showing (**a**) net power production and (**b**) warm surface seawater temperature (solid line) and cold deep-sea water temperature (dashed line). All plants in the shown countries are sized for a nominal gross power output of 136 MW_{gross}

(Banerjee et al. 2017) or ammonia (Martel et al. 2012), or the enhancement of thermal resources from solar thermal power (Straatman and van Sark 2008). It remains to be seen whether the benefits of several power and commodity flows outweigh the drawbacks from increased system complexity and cost.

3.3 The impact of ocean thermal energy resources on power production profiles and plant design

In our earlier work (Langer et al. 2022a), we already assessed the impact of ocean thermal energy resources on OTEC's power production and plant design, but only for four plants in Indonesia. In this subsection, we validate and further refine our earlier findings with global results.

In literature, OTEC is considered a steady and stable baseload generator (Martel et al. 2012; Vega 2012; Thirugnana et al. 2021). Figure 6 examines this further and shows the impact of ocean thermal energy resources on net power production, exemplified for 136 MW_{gross} plants in four regions. We show that the shape of OTEC's power production profile is mainly determined by the surface seawater temperature, whereas its magnitude is mainly determined by the deep-sea water temperature. The former observation is apparent for Japan, where the net power production profile follows the seasonal changes of surface seawater temperature more closely than the other profiles do. The latter observation becomes clear when comparing the cases of India and Puerto Rico. Although the surface seawater temperature tends to be higher in India than in Puerto Rico, the net power production in India is lower. This is because the deep-sea water temperature in India is roughly 2 °C higher than the one in Puerto Rico. Given the consequent lower temperature range between evaporator and condenser as well as the increased deep-sea water pumping power, the plant in India needs more working fluid and deep-sea water to produce the same net power as the plant in Puerto Rico, which results in a lower net efficiency.

Figure 7 maps the temperature configurations with the lowest LCOE across the world. The map only displays configurations with an occurrence of more than 1%. As shown in Fig. 8, 79.6% of all analysed sites are designed with configuration 1 (minimum surface and maximum deep-sea water temperature), followed by configuration 2 (median surface and maximum deep-sea water temperature) with 14.2%.

Based on Fig. 9, we deduce several rules for sizing OTEC plants economically. The warm system side tends to be sized for minimum warm seawater temperature (i.e., configurations 1, 4, and 7) if the maximum warm seawater temperature is at least 25 °C with seasonal fluctuations of 10 °C or less. If the surface seawater is cooler and/or more fluctuating throughout the year, pyOTEC tends to size the warm system side for median warm seawater temperatures (mainly configuration 2) as a more conservative design either incurs too high costs or returns infeasible plant designs (i.e., pumping power > gross power output). From the cold system side, we observe that plants tend to be designed less conservative, the lower the minimum cold seawater temperature and its fluctuations are.

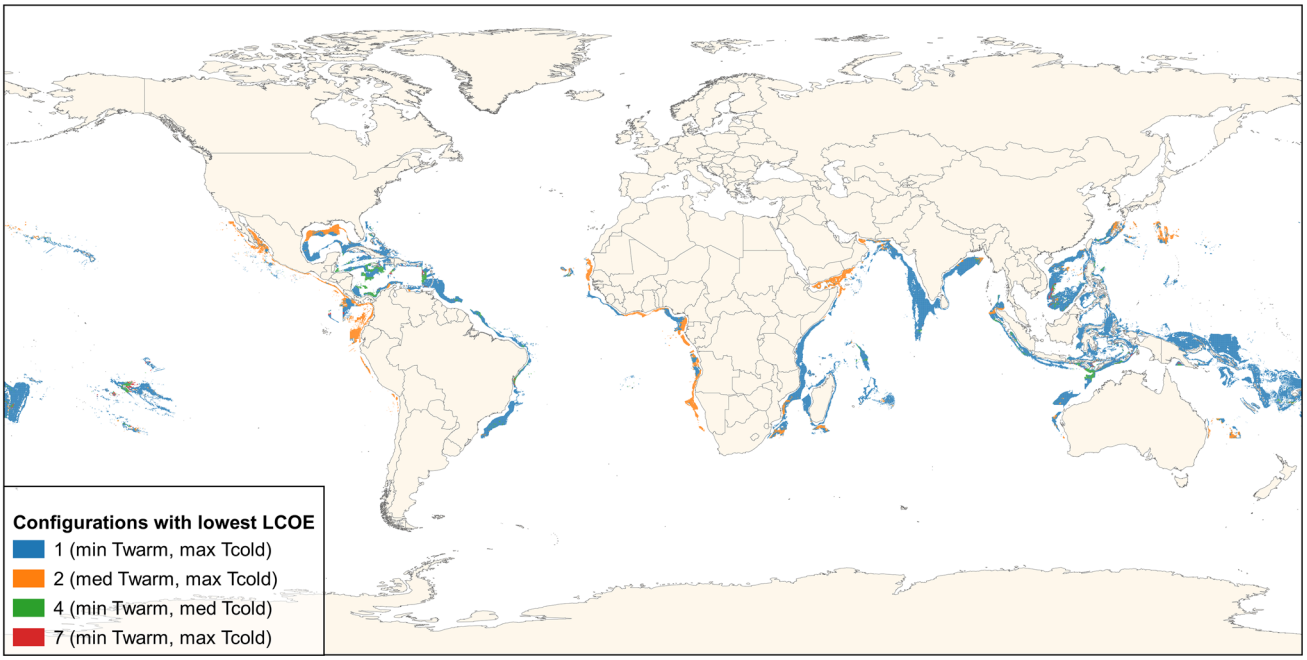

Fig. 7 Configurations yielding the lowest off-design LCOE across the world under low-cost assumptions ($N = 162{,}620$ sites). T_{warm} in the legend refers to the warm surface seawater temperature; T_{cold} refers to the cold deep-sea water temperature

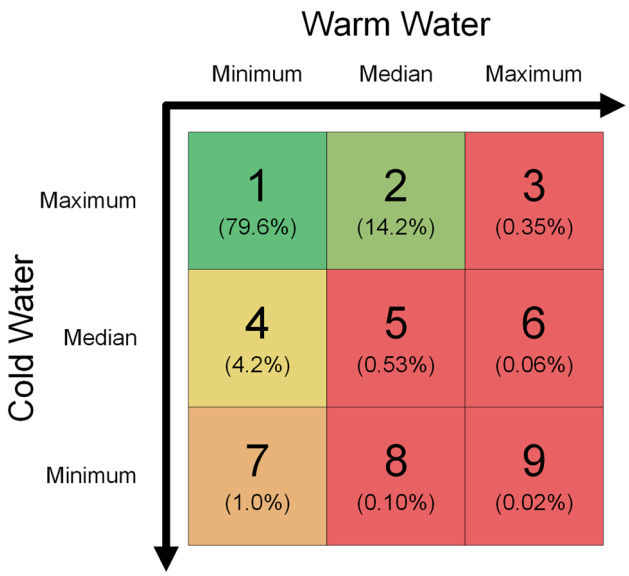

Fig. 8 Design configurations and the percentage of them returning the lowest off-design LCOE ($N = 162{,}620$ sites). The cells above are coloured from red to green based on increasing percentage

These findings mostly harmonise with our earlier work (Langer et al. 2022a) for Indonesia, where we concluded that conservative system designs show the best economic performance. Against our earlier results, we did find sites at which the less conservative configurations 3, 6, and 9 yielded the lowest LCOE. However, such cases are rare with a combined occurrence of 0.43% across the global sample. Therefore, we see our earlier findings validated and consolidated for global application, at least under the used technical and economic assumptions.

3.4 Sensitivity analysis

Figure 10 displays the results of the sensitivity analysis for the sites in Indonesia ($N = 14{,}422$ sites). The LCOE is most sensitive to changes in availability factor a_f and discount rate r, which underlines the importance of reliable operation and sound financing if the discount rate represents weighted average cost of capital, for example. Out of all cost components, structure and mooring costs are most impactful, which might motivate further research into onshore OTEC, which does not incur these costs. Moreover, the LCOE is moderately sensitive to technical parameters, like overall heat transfer coefficient U, pressure drop coefficient K_L, and hydraulic seawater pump efficiency $\eta_{pump,hyd}$.

Regarding the configuration, we observe that the overall composition persists across all studied parameters: The most conservative configuration 1 (minimum warm seawater temperature, maximum cold seawater temperature) is selected most often, followed by the less conservative configuration 4 (minimum warm seawater temperature, median cold seawater temperature). Configuration 1 becomes even more dominant the worse the underlying technical parameters are, most visibly for the hydraulic seawater pump efficiency $\eta_{pump,hyd}$ and pressure drop coefficient K_L (note the latter's inverse effect). Configuration 1 is dominant, because

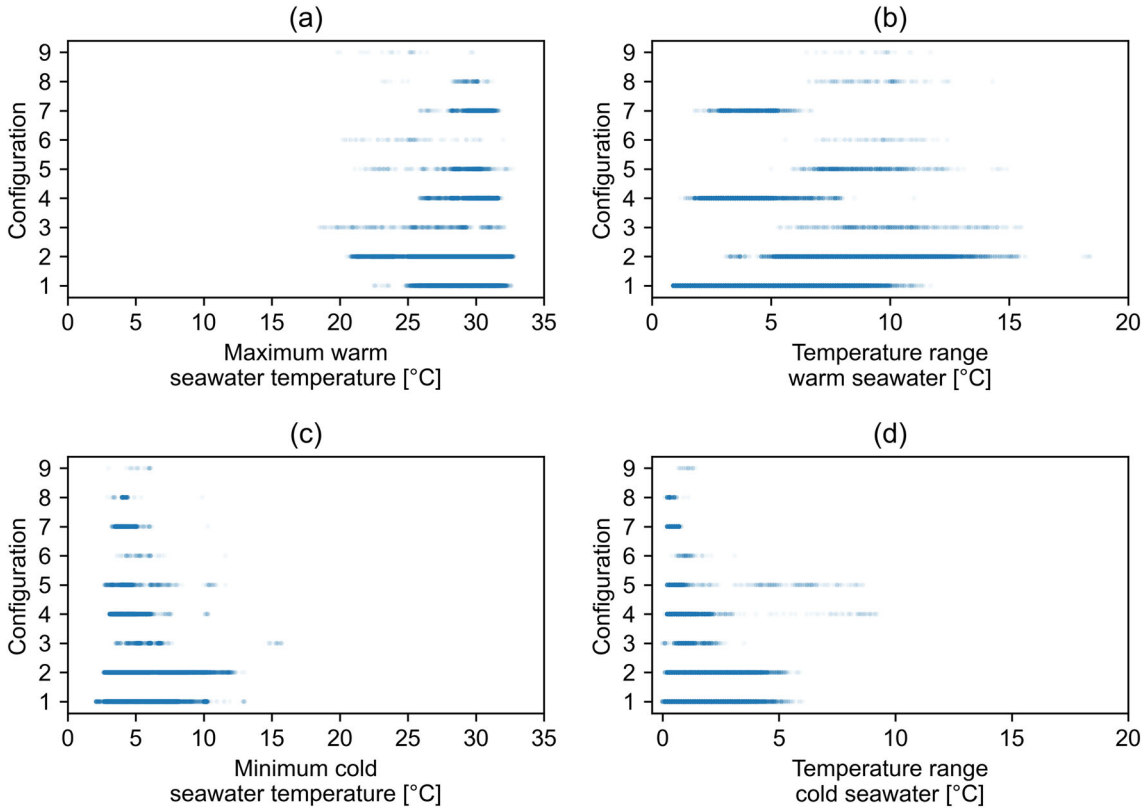

Fig. 9 The configurations yielding the lowest off-design LCOE of all analysed OTEC plants ($N = 162{,}620$ sites) plotted against the minimum seawater temperature and temperature range; (**a**, **b**) refer to the warm surface seawater temperature, (**c**, **d**) refer to the cold deep-sea water temperature. The temperature range is the difference between maximum and minimum seawater temperature throughout the modelled time horizon and reflects the variability of ocean thermal energy resources at the studied sites

oversizing OTEC plants contributes to a stable baseload generation to recover the plants' CAPEX; and worse technical system parameters seem to reinforce this effect. Out of all cost components, structure and mooring as well as pipe costs are most impactful, albeit in opposite directions. In our cost model, structure and mooring costs depend on the plant's gross power output and not on configuration. For these costs, configuration 1 becomes less dominant as fewer costs need to recovered, thus making baseload generation less important. Pipe costs, in contrast, depend on the dimensions and amount of pipes and vary per configuration. With lower pipe costs, oversizing the pipes becomes cheaper, thus making configuration 1 even more attractive. The scaling exponents b reflecting OTEC's economies of scale do not affect the composition of configurations significantly.

The observations above consolidate our earlier and present findings, namely that conservative plant designs tend to return the lowest LCOE.

4 Conclusion

This paper presents the open-source model pyOTEC, which designs *Ocean Thermal Energy Conversion (OTEC)* plants for best economic performance across large regional scopes using spatiotemporally resolved ocean thermal energy resource data. Sites for OTEC deployment are based on a site selection analysis using exclusion criteria like water depth, marine protected areas, and exclusive economic zones. We apply pyOTEC to more than 100 countries and territories with technically feasible OTEC sites and design more than 150,000 plants to assess OTEC's global economic potential. This paper contributes to the research field by (1) providing the first global assessment of economic OTEC resources, (2) showing the impact of availability and seasonality of ocean thermal energy resources on OTEC's technical and economic performance, (3) validating and consolidating global OTEC design guidelines, and (4) generating spatially and temporally explicit net power production profiles for energy system optimisation models.

Our results show that more than 107 PWh/year could be generated globally with OTEC, although this potential might

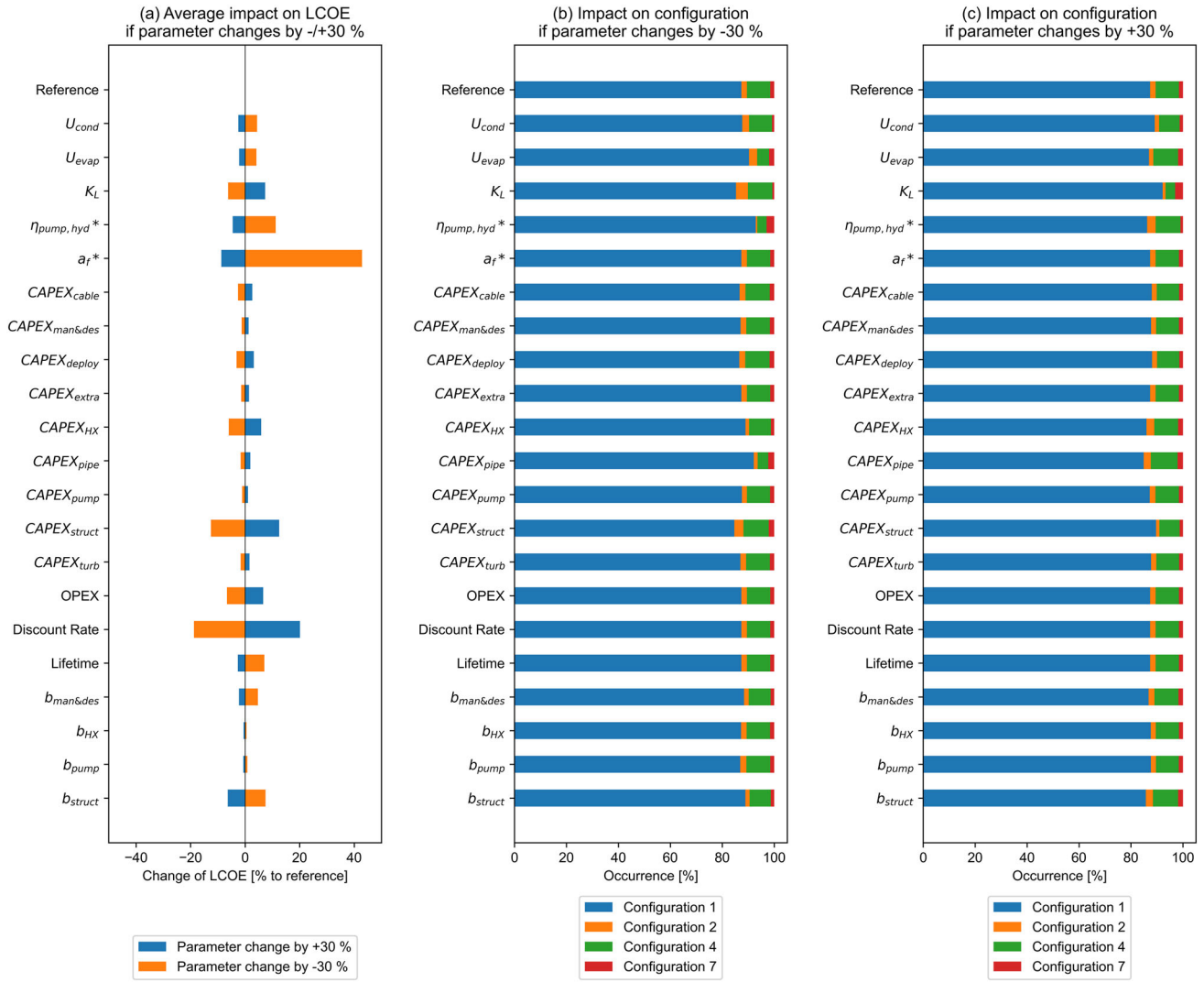

Fig. 10 The sensitivity of LCOE and configuration of 136 MW_{gross} plants in Indonesia ($N = 14{,}422$ sites) to changes in technical and economic parameters by $-/+30\%$. Parameters marked with * could not be increased by $+30\%$ beyond 100% and are instead capped at 100%. See abbreviations table for meaning of symbols and indices

be less if more advanced negative environmental and economic impacts were considered. LCOEs tend to be the lowest along the equator in South-East Asia and South America, and higher in Africa, East Asia, and Australia. If fully scaled to 136 MW_{gross}, OTEC can also be economically attractive in the latter regions with LCOEs below 20 US¢(2021)/kWh. Small-scale systems also show economic potential as seen for small island developing states. These islands are OTEC's most relevant niche as systems below 10 MW_{gross} could fully and cost-effectively substitute Diesel generators, which might be more challenging with other renewables due to limited land availability, amongst others. The global analysis shows that in most cases, the best economic performance is achieved if systems are designed conservatively based on worst-case surface and deep-sea water temperatures. The warm system side tends to be designed conservatively if the maximum surface seawater temperature is above 25 °C and fluctuates by less than 10 °C throughout the year. The cold system side tends to be designed more conservatively with warmer and more fluctuating deep-sea water temperatures. The preferrence of conservatively designed OTEC plants has been tested and validated via a sensitivity analysis for Indonesia, which revealed the availability factor and discount rate as the most influental inputs for the LCOE. For the selected configuration, the hydraulic seawater pump efficiency and pipe costs are most impactful, although the overall composition of preferred configurations only changes slightly.

We conclude that OTEC is a technically and economically intriguing technology despite its relatively high current LCOE compared to the ones of other renewables. Right now,

it seems like most countries put their hopes on solar photovoltaics, wind power, and battery storage to master the energy transition. However, just like in finance, we believe that diversification is an essential element of power systems. With this in mind, we hope that the world learns to appreciate OTEC's merits and starts promoting its commercialisation. After all, it would not only be the communities of small island states that could benefit from clean, stable, and affordable OTEC electricity, but also the ones of large continental coastal states.

Acknowledgements The work reported in this paper is partly funded by a grant from the Dutch research council NWO for the project entitled "Regional Development Planning and Ideal Lifestyle of Future Indonesia", under the NWO Merian Fund call on collaboration with Indonesia. Many thanks to Carlos Infante Ferreira and Kamel Hooman for their critical and insightful feedback. This study has been conducted using E.U. Copernicus Marine Service Information; https://doi.org/10.48670/moi-00021.

Author contributions JL: conceptualization; data curation; formal analysis; investigation; methods & materials; original draft. KB: contributions to methodology; supervision; methods & materials; validation; writing—review & editing.

Data availability pyOTEC is publicly available under https://github.com/JKALanger/pyOTEC, and analysed sites as well as their average net power production profiles per studied regions can be downloaded under https://doi.org/10.4121/65585fc3-4ed3-4c08-83ef-adbbc7300582.

Declarations

Conflict of interest The authors declare no competing interest.

Appendix

Setting up pyOTEC

Here, we describe how to set up pyOTEC. First, we recommend users to install the latest version of Anaconda as it contains most of the libraries used by pyOTEC. Then, the netCDF4 library needs to be installed via Anaconda prompt. Next, the pyOTEC repository needs to be downloaded from GitHub (https://github.com/JKALanger/pyOTEC). Before using pyOTEC, the user needs to register and create an account at Copernicus Marine Service (2022) and install the Python package *motuclient*. The account credentials (username and password) are needed for authentication and can either be hardcoded in pyOTEC or stored in a separate callable file. The MOTU API is needed to automatically request and download the data as *"nc files"* (a standard data format that allows for the efficient storage of large datasets resolved in space and time). Then, the user opens the file pyOTEC.py in their preferred Python IDE, e.g., Spyder. To start the analysis, the user needs to provide the region and plant size as gross power output. If the user wants to check and change the inputs used by pyOTEC, they can do so in the files parameters_and_constants.py and capex_opex_lcoe.py.

Processing of seawater temperature data

After the successful download of the seawater temperature data, pyOTEC processes the data further. The data of the raw nc files spread over the rectangular shape of the region's geographical extent, thus also covering land areas and marine areas unsuitable for OTEC. pyOTEC checks the coordinates of the raw temperature profiles with the coordinates of the technically feasible OTEC sites mapped in Sect. 2.2, and discards the profiles with no match. Then, outliers and faulty values in the profiles (e.g., negative temperatures) are replaced by NaN. Here, we define outliers as values that are more than three times the interquartile range away from the profiles' minima and maxima. In Langer et al. (2022a), we used a factor of 1.5 for Indonesia, but after trial-and-error with the more extensive and diverse global temperature datasets, we found a factor 3 to be more suitable for removing outliers without removing rare, but not impossible, extreme temperature values. Outliers are detected using a 1-month rolling time window. All NaN are filled via linear interpolation. The processed temperature profiles and design values for each OTEC site are stored as h5 files (an open-source data format that allows for the storage of several large datasets in one file).

References

Ascari MB, Hanson HP, Rauchenstein L, Van Zwieten J, Bharathan D, Heimiller D, Langle N, Scott GN, Potemra J, Nagurny NJ, Jansen E (2012) Ocean thermal extractable energy visualization: final technical report. Lockheed Martin Mission Systems & Sensors (MS2), Manassas

Asian Development Bank (2016) Sector assessment (summary): energy. Asian Development Bank, Mandaluyong City

Banerjee S, Musa MN, Jaafar AB (2017) Economic assessment and prospect of hydrogen generated by OTEC as future fuel. Int J Hydrog Energy 42:26–37. https://doi.org/10.1016/j.ijhydene.2016.11.115

Bernardoni C, Binotti M, Giostri A (2019) Techno-economic analysis of closed OTEC cycles for power generation. Renew Energy 132:1018–1033. https://doi.org/10.1016/j.renene.2018.08.007

Bharathan D (2011) Staging rankine cycles using ammonia for OTEC power production. National Renewable Energy Laboratory, Golden

Bosch J, Staffell I, Hawkes AD (2019) Global levelised cost of electricity from offshore wind. Energy. https://doi.org/10.1016/j.energy.2019.116357

Brown T, Hörsch J, Schlachtberger D (2018) PyPSA : python for power system analysis. J Open Res Softw. https://doi.org/10.5334/jors.188

Cable B (2010) NAVFAC ocean thermal energy conversion (OTEC) project. Lockheed Martin Mission Systems & Sensors (MS2), Manassas

DTU Wind Energy, The World Bank Group (2021) Vortex, energy sector management assistance program data obtained from the global wind atlas 3.0. https://globalwindatlas.info/. Accessed 13 Sep 2021

Du T, Jing Z, Wu L, Wang H, Chen Z, Ma X, Gan B, Yang H (2022) Growth of ocean thermal energy conversion resources under greenhouse warming regulated by oceanic eddies. Nat Commun. https://doi.org/10.1038/s41467-022-34835-z

E.U. Copernicus Marine Service Infortmation (CMEMS) (2022) Global ocean physics reanalysis. https://data.marine.copernicus.eu/product/GLOBAL_MULTIYEAR_PHY_001_030/description. Accessed 4 Apr 2023

EIA Electricity. https://www.eia.gov/international/data/world/electricity/electricity-consumption?pd=2&p=0000002&u=0&f=A&v=mapbubble&a=-&i=none&vo=value&t=C&g=0000000000000000000000000000000000000000001&l=249-ruvvvvfvtvnvv1vrvvvvfvvvvvvfvvvou20evvvvvvvvvvnvvvs0008. Accessed 4 Apr 2023

GEBCO Bathymetric Compilation Group 2022 (2022) The GEBCO_2022 Grid—a continuous terrain model of the global oceans and land. https://www.gebco.net/data_and_products/gridded_bathymetry_data/. Accessed 4 Apr 2023

Giostri A, Romei A, Binotti M (2021) Off-design performance of closed OTEC cycles for power generation. Renew Energy 170:1353–1366. https://doi.org/10.1016/j.renene.2021.02.047

Hall K, Kelly S, Henry L (2022) Site selection of ocean thermal energy conversion (OTEC) plants for barbados. Renew Energy 201:60–69. https://doi.org/10.1016/j.renene.2022.11.049

Hammar L, Gullström M, Dahlgren TG, Asplund ME, Goncalves IB, Molander S (2017) Introducing ocean energy industries to a busy marine environment. Renew Sustain Energy Rev 74:178–185. https://doi.org/10.1016/j.rser.2017.01.092

International Renewable Energy Agency (2020) Innovation outlook: ocean energy technologies. International Renewable Energy Agency, Abu Dhabi

International Renewable Energy Agency (2022) Renewable power generation costs in 2021. International Renewable Energy Agency, Jakarta

International Renewable Energy Agency, International Geothermal Association (2023) Global geothermal market and technology assessment. International Renewable Energy Agency, Abu Dhabi

Jia Y, Nihous GC, Rajagopalan K (2018) An evaluation of the large-scale implementation of ocean thermal energy conversion (OTEC) using an ocean general circulation model with low-complexity atmospheric feedback effects. J Mar Sci Eng. https://doi.org/10.3390/jmse6010012

Jung J-Y, Lee HS, Kim H-J, Yoo Y, Choi W-Y, Kwak H-Y (2016) Thermoeconomic analysis of an ocean thermal energy conversion plant. Renew Energy 86:1086–1094. https://doi.org/10.1016/j.renene.2015.09.031

Langer J, Quist J, Blok K (2020) Recent progress in the economics of ocean thermal energy conversion: critical review and research agenda. Renew Sustain Energy Rev 130:109960. https://doi.org/10.1016/j.rser.2020.109960

Langer J, Cahyaningwidi AA, Chalkiadakis C, Quist J, Hoes O, Blok K (2021) Plant siting and economic potential of ocean thermal energy conversion in Indonesia a novel GIS-based methodology. Energy 224:120121. https://doi.org/10.1016/j.energy.2021.120121

Langer J, Infante Ferreira C, Quist J (2022a) Is bigger always better? Designing economically feasible ocean thermal energy conversion systems using spatiotemporal resource data. Appl Energy 309:118414. https://doi.org/10.1016/j.apenergy.2021.118414

Langer J, Quist J, Blok K (2022b) Upscaling scenarios for ocean thermal energy conversion with technological learning in Indonesia and their global relevance. Renew Sustain Energy Rev 158:112086. https://doi.org/10.1016/j.rser.2022.112086

Liu T, Hirose N, Yamada H, Ikegami Y (2020) Estimation of ocean thermal energy potential in the Aguni Basin. Appl Ocean Res 101:102185. https://doi.org/10.1016/j.apor.2020.102185

Marineregions (2020) Marine and land zones: the union of world country boundaries and EEZ's - Version 3. https://www.marineregions.org/downloads.php. Accessed 4 Apr 2023

Martel L, Smith P, Rizea S, Van Ryzin J, Morgan C, Noland G, Pavlosky R, Thomas M, Halkyard J (2012) Ocean thermal energy conversion life cycle cost assessment. Final Technical Report. Lockheed Martin, Washington, D.C., USA

Michalena E, Hills JM (2018) Paths of renewable energy development in small island developing states of the South Pacific. Renew Sustain Energy Rev 82:343–352. https://doi.org/10.1016/j.rser.2017.09.017

Nihous GC (2005) An order-of-magnitude estimate of ocean thermal energy conversion resources. J Energy Resour Technol 127:328–333. https://doi.org/10.1115/1.1949624

Nihous GC (2007) A preliminary assessment of ocean thermal energy conversion resource. J Energy Resour Technol 129:10–17. https://doi.org/10.1115/1.2424965

Pfenninger S, Pickering B (2018) Calliope: a multi-scale energy systems modelling framework. J Open Source Softw 3:825. https://doi.org/10.21105/joss.00825

QGIS.org (2023) QGIS geographic information system. http://www.qgis.org. Accessed 18 Sep 2023

Rajagopalan K, Nihous GC (2013) Estimates of global ocean thermal energy conversion (OTEC) resources using an ocean general circulation model. Renew Energy 50:532–540. https://doi.org/10.1016/j.renene.2012.07.014

Sharqawy MH, Lienhard VJH, Zubair SM (2011) Thermophysical properties of seawater: a review of existing correlations and data. Desalin Water Treat 29:355–355. https://doi.org/10.5004/dwt.2011.2947

Sinnott R, Towler G (2022) Chemical engineering design, 3rd edn. Elsevier, Amsterdam

Soto R, Vergara J (2014) Thermal power plant efficiency enhancement with ocean thermal energy conversion. Appl Therm Eng 62:105–112. https://doi.org/10.1016/j.applthermaleng.2013.09.025

Straatman PJT, van Sark WGJHM (2008) A new hybrid ocean thermal energy conversion-Offshore solar pond (OTEC-OSP) design: a cost optimization approach. Sol Energy 82:520–527. https://doi.org/10.1016/j.solener.2007.12.002

Thirugnana ST, Jaafar AB, Yasunaga T, Nakaoka T, Ikegami Y, Su S (2021) Estimation of ocean thermal energy conversion resources in the east of malaysia. J Mar Sci Eng 9:1–11. https://doi.org/10.3390/jmse9010022

UNEP-WCMC (2023a) Protected Area Profile for Africa from the World Database on Protected Areas. https://www.protectedplanet.net/region/AF. Accessed 4 Apr 2023

UNEP-WCMC (2023b) Protected Area Profile for Asia & Pacific from the World Database on Protected Areas. https://www.protectedplanet.net/region/AS. Accessed 4 Apr 2023

UNEP-WCMC (2023c) Protected Area Profile for Latin America & Caribbean from the World Database on Protected Areas. https://www.protectedplanet.net/region/SA. Accessed 4 Apr 2023

UNEP-WCMC (2023d) Protected Area Profile for North America from the World Database on Protected Areas. https://www.protectedplanet.net/region/NA. Accessed 4 Apr 2023

Upshaw CR (2012) Thermodynamic and Economic Feasibility Analysis of a 20 MW Ocean Thermal Energy Conversion (OTEC) Power. Master Thesis, University of Texas at Austin

Vega LA (2010) Economics of ocean thermal energy conversion (OTEC): an update. Offshore Technol Conf. https://doi.org/10.4043/21016-MS

Vega LA (2012) Ocean thermal energy conversion. Encycl Sustain Sci Technol 2:7296–7328

Vega LA, Michaelis D (2010) First generation 50 MW OTEC plantship for the production of electricity and desalinated water. Proc Annu Offshore Technol Conf 4:2979–2995. https://doi.org/10.4043/20957-ms

Vera D, Baccioli A, Jurado F, Desideri U (2020) Modeling and optimization of an ocean thermal energy conversion system for remote islands electrification. Renew Energy 162:1399–1414. https://doi.org/10.1016/j.renene.2020.07.074